Available online at www.sciencedirect.com
SCIENCE DIRECT®
Coordination Chemistry Reviews 249 (2005) 1316–1326
COORDINATION CHEMISTRY REVIEWS
www.elsevier.com/locate/ccr

Review

Oxygen and hydrogen photocatalysis by two-electron mixed-valence coordination compounds

Joel Rosenthal, Julien Bachman, Jillian L. Dempsey, Arthur J. Esswein, Thomas G. Gray, Justin M. Hodgkiss, David R. Manke, Thomas D. Luckett, Bradford J. Pistorio, Adam S. Veige, Daniel G. Nocera *

Department of Chemistry, 6-335, Massachusetts Institute of Technology, 77 Massachusetts Avenue, Cambridge, MA 02139-4307, USA

Received 24 September 2004; accepted 22 March 2005
Available online 8 June 2005

Contents

Abstract

Two-electron mixed valency is a useful design concept for hydrogen and oxygen photocatalysis. As single-electron mixed-valence compounds react in one-electron steps, two-electron mixed-valence compounds may react in two-electron steps at the constituent redox sites, whether they are metal- or ligand-based. With the redox centers working in concert upon photoexcitation, two- and four-electron transformations are promoted along excited-state pathways. Such a strategy is ideally suited to the activation of small molecules. We describe the photochemistry for hydrogen and oxygen activation using two-electron mixed-valence complexes of three different motifs: (a) M^n–M^{n+2} bimetallic complexes, (b) tetrapyrrole macrocycles and (c) externally bridged di-iron(III) μ-oxo porphyrin dimers.

Keywords: Hydrogen; Oxygen; Photocatalysis; Valence; Multielectron; Solar; Proton-coupled electron transfer

1. Introduction

The activation and use of small molecules of energy consequence, including CO_2, N_2 and CH_4 in addition to H_2, H_2O and O_2, share basic chemical commonalities [1]. They are all *multielectron* processes [2–4]. Moreover, for the small

* Corresponding author. Tel.: +1 617 253 5537; fax: +1 617 253 7670.
E-mail address: nocera@mit.edu (D.G. Nocera).

0010-8545/$ – see front matter © 2005 Elsevier B.V. All rights reserved.
doi:10.1016/j.ccr.2005.03.034

molecules listed above, proton transfer must accompany electron transfer [5–14], as both *electron and proton inventories* need to be managed for successful small molecule activation [15–19]. Additionally, small molecule transformations confront sizable thermodynamic or kinetic barriers to *bond activation* that must be overcome from electronic excited states if an energy-storing catalytic cycle is to be closed.

Our research efforts have addressed the italicized research themes of the foregoing paragraph by expanding the reactivity of metal complexes in electronic excited states beyond conventional one-electron transfer. Much of the work has been devoted to the concept of two-electron mixed valency. The approach is straightforward: as single-electron mixed-valence compounds react in one-electron steps [20,21] two-electron mixed-valence compounds may react in two-electron steps at the constituent redox sites, whether they are metal- or ligand-based. This approach does not demand that each metal react in a concerted two-electron step, rather, it requires the one-electron mixed-valence species to be kinetically or thermodynamically unstable with respect to the two-electron species. In this manner, even if the primary photoevent involves single electron transfer, an ensuing redox event will be facile, thus driving net multielectron reactivity.

The types of two-electron mixed valency that we are currently investigating are represented schematically in Scheme 1: (a) bimetallic complexes that rely on ligand sets favoring a ground-state M^n–M^{n+2} species, which is stabilized relative to its comproportionated and symmetric $M^{n+1}\cdots M^{n+1}$ congener; (b) porphyrinogens that store two-electron equivalency in the framework of a macrocyclic ligand; and (c) M^{III}–O–M^{III} macrocycles tethered to a rigid spacer that upon excitation produce a two-electron mixed-valence metal-oxo intermediate, which is a reactive oxidant. In each case, the two-electron mixed-valence complex is the critical intermediate for promoting discrete two- and four-electron transformations. Recent results in areas (a)–(c) are described in detail below.

2. Two-electron mixed-valence bimetallic complexes

2.1. Hydrogen production using two-electron mixed-valence photocatalysts

The two-electron mixed-valence approach is ideally suited to manage the two-electron chemistry of hydrogen production and activation. Although the occurrence of authentic M^n–M^{n+2} compounds is uncommon [22], such complexes can be stabilized by ligand frameworks that juxtapose π-accepting groups directly adjacent to π-donating groups. One such construct is embodied by bis(difluorophosphino)methylamine (dfpma, $CH_3N(PF_2)_2$) and bis(bistrifluoroethoxyphosphino)methylamine (tfepma, $CH_3N[P(OCH_2CF_3)_2]_2$) ligand sets that place an amine bridgehead between two electron-deficient phosphines (PR^F_2) or phosphites ($P(OR^F)_2$). These diphosphazane ligands are distinguished by their ability to drive the internal disproportionation of binuclear $M_2^{I,I}$ cores to $M_2^{0,II}$ cores [23] for the metals rhodium [24,25] and iridium [26–28]. X-ray crystal structures reveal a pronounced asymmetry in the diphosphazane framework upon ligation to a bimetallic core [24]. The result is consistent with asymmetric donation of the amine bridgehead lone pair to the PR^F_2 bonded to M^{II}. With $M^{II} \rightarrow PR^F_2$ π-backbonding diminished, the PR^F_2 group acts as a σ-donor to stabilize the high-valent M^{II} metal center. Correspondingly, with the nitrogen lone pair electron density channeled away from the second neighboring PR^F_2 group, its strong π-accepting properties are maintained and hence M^0 is stabilized. In this manner, we believe that the dfpma and tfepma ligands accommodate the intramolecular disproportionation of $M_2^{I,I}$ to $M_2^{0,II}$.

The benefit of designing authentic two-electron mixed-valence complexes is the ability to effect multielectron redox chemistry among discrete molecular species. With the metals working in concert, two- and four-electron transformations are promoted along ground- and excited-state pathways. As shown in Scheme 2, hydrogen halides react with $Rh_2^{0,0}(dfpma)_3L_2$ (L = PPh_3) in discrete two-electron steps to afford the LRh^0–$Rh^{II}X_2$ and X_2Rh^{II}–$Rh^{II}X_2$ congeners, respectively [24]. An equivalent of H_2 is produced in each step. By incorporating the same $d\sigma^*$ excited state within the electronic structure of the LRh^0–Rh^0L, LRh^0–$Rh^{II}X_2$ and X_2Rh^{II}–$Rh^{II}X_2$ cores [29–32], interconversion among the series members may be accomplished by the elimination of halogen in two-electron steps [24,25]. The LRh^0–Rh^0L starting complex can be regenerated as long as a halogen trap is present, thus permitting the photocycle shown in Fig. 1 to be constructed [33]. In brief, a sacrificial photon removes an axial CO from the $Rh_2^{0,0}$ complex, opening a coordination site for HX attack (the axial site may also be opened thermally). Disappearance of the $Rh_2^{0,0}$ complex is accompanied by the formation of 1 equiv. of H_2 and the appearance of a blue species that eventually converts to the LRh^0–$Rh^{II}X_2$ complex. Photoactivation of the Rh^{II}–X bond enables the photocycle to be closed.

2.2. Hydrides related to two-electron mixed valence cores

Hydrogen elimination is facile and neither hydrido- nor hydrido-halide intermediates are observed during turnover of the photocycle shown in Fig. 1. With the goal of characterizing hydride species of two-electron mixed-valence cores and understanding their dihydrogen chemistry, we turned our attention to di-iridium complexes owing to the increased stability of third-row metal-hydride bonds relative to their second-row counterparts. Our findings, summarized in Fig. 2 for an $Ir_2^{0,II}$ core ligated by tfepma, establish that two-electron mixed-valence bimetallic cores are able to support hydrides and hydrido-halides, and that these species are of consequence to HX photocatalysis [26]. An especially surprising result is the facility with which H_2

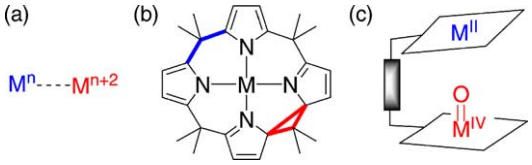

Scheme 1.

is able to add to and eliminate from a M^n–M^{n+2} complex. As shown for the conversion of **1** to **2**, the unusual circumstance of *reversible* hydrogenation of the metal–metal bond is observed.

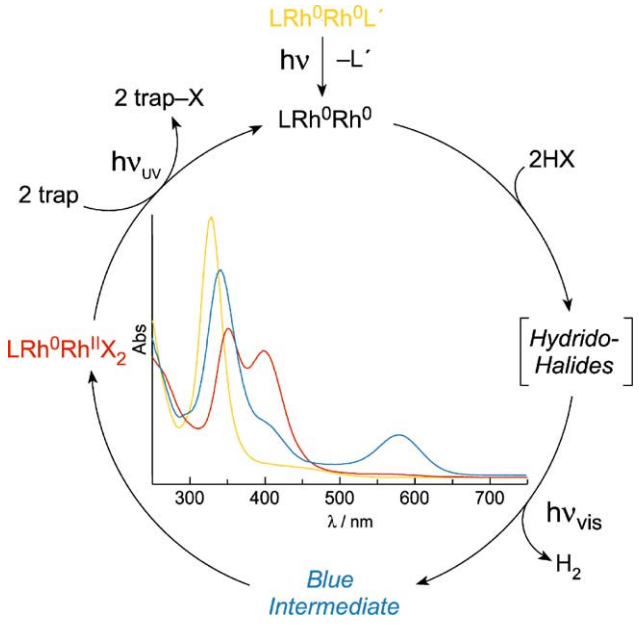

Fig. 1. The photocycle for H_2 production from homogeneous solutions of HX using a two-electron mixed-valence dirhodium photocatalyst. The $Rh_2^{0,II}$ core is strapped by three dfpma ligands.

Application of the tfepma ligand to dirhodium cores permits the unanticipated isolation of stable dihydride–dihalide complexes of rhodium (as opposed to the situation shown in Scheme 1 for dirhodium cores ligated by the dfpma ligand) [34]. The structure of one such complex is shown in Fig. 3, which displays a syn disposition of the two hydrides about a $Rh_2^{II,II}$ core. The reasons why changing the phosphorus substituent from –F to the bulkier $–OCH_2CF_3$ on the bridging diphosphazane allows for the synthesis and isolation of the dihydride remain unclear. Notwithstanding, such compounds are providing additional insights with regard to the mechanism of the photocycle in Fig. 1. Given that the dihydrides are the primary products of HX addition to $Rh_2(tfepma)_3L_2$, one can surmise that the hydrido-halide intermediate of the H_2 photocycle depicted in Fig. 1 resembles the complex of Fig. 3 in basic form and structure. Evidence for this assignment stems from the photoreactivity of the $Rh_2^{II,II}$ dihydride dihalide. Upon photolysis, the compound promptly produces H_2 and a metal complex possessing absorption features coincident with those of the previously unidentified blue intermediate, whose absorption spectrum is shown in the inset of Fig. 1. Preliminary structural and spectroscopic results indicate that the blue intermediate is the $Rh_2^{I,I}Cl_2$ complex expected from H_2 reductive photoelimination from the *syn* complex. Subsequent conversion of the $ClRh^I\cdots Rh^ICl$ core to Rh^0–$Rh^{II}Cl_2$ by an intramolecular rearrangement places the dihydride on the photocycle pathway shown in Fig. 1.

2.3. Mechanism of hydrogen production

Experimental and computational studies of the hydrides presented in the foregoing section provide an emerging picture for reactivity and management of H_2 at M^n–M^{n+2} cores [35]. Hydrogen attack and elimination occurs at the M^{n+2} end of the bimetallic core and is mediated by a bridging hydride, as shown in Fig. 4 for the reaction of H_2 at a

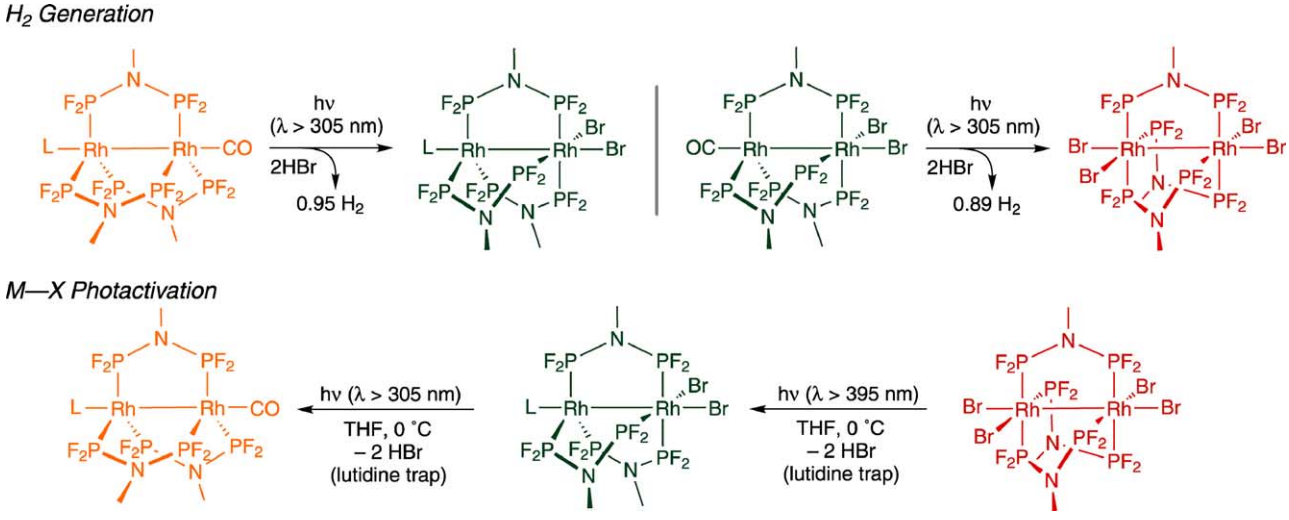

Scheme 2.

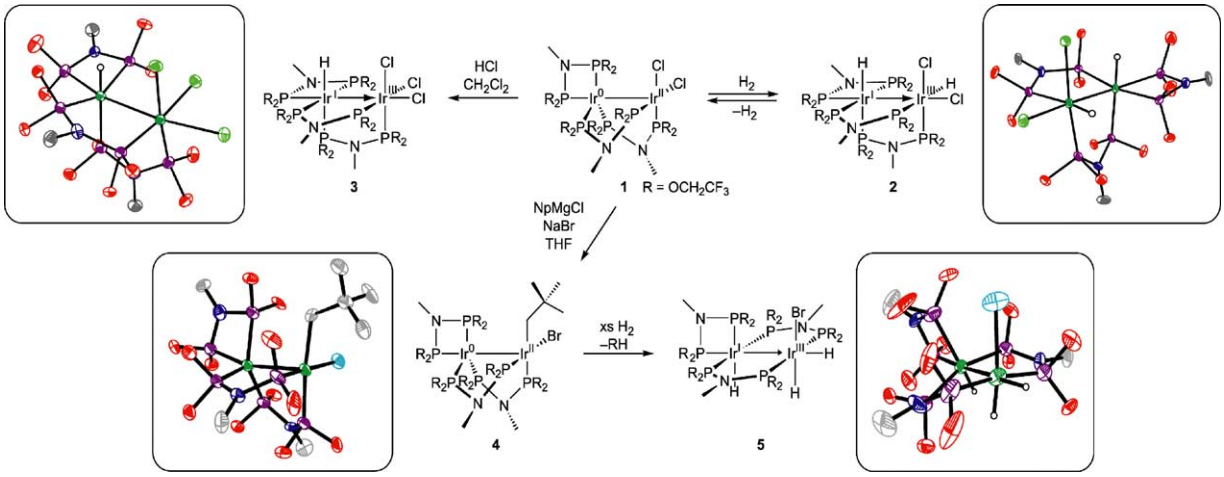

Fig. 2. Hydride and hydrido-halo chemistry of two-electron mixed-valence di-iridium complexes.

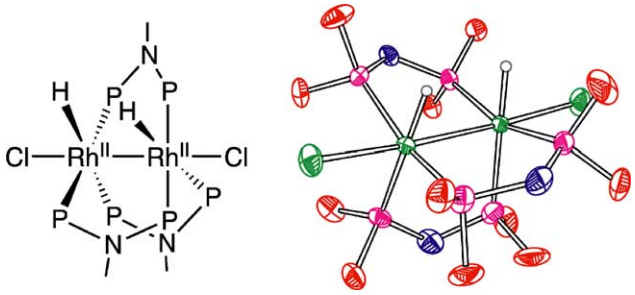

Fig. 3. A "syn" dihydride–dihalide complex of dirhodium resulting from H_2 addition to $Rh_2^{0,II}$tfepma$_3$Cl$_2$ with thermal ellipsoids drawn at the 50% probability level. The species is relevant to the HX oxidative-addition product of the H_2 photocycle shown in Fig. 1.

Ir^0–$Ir^{II}(X)_2$ core. Addition of H_2 to the axial site *trans* to the metal-metal bond is unproductive. To position a hydrogen atom for transfer to the neighboring Ir^0 center, an equatorial halide ligand must swing into the axial coordination site. Once residing in the equatorial coordination site, a hydrogen atom easily migrates into a position bridging the two iridium centers. This represents the transition state that directly leads to the terminal dihydride product. For addition to Ir^0–$Ir^{II}(X)_2$ cores, the bridging hydride must come from the HX or H_2 reactant. As shown in Scheme 3 for the "Swing" mechanism, this leads to the *fac* stereochemistry observed in Fig. 2 for the addition of H_2 and HCl to **1**, yielding **2** and **3**, respectively. A similar bridging state prevails for hydrogen atom migration at Ir^0–Ir^{II}(H)(X) cores [36], which may be generated by the addition of a single equivalent of H_2 to **4** in Fig. 2. The terminal hydride (H_a in Scheme 3, "Fold") that is present from the outset smoothly folds into the bridging position as hydrogen attacks the axial coordination site to give product **5** (Fig. 2) with *mer* stereochemistry about the Ir^{III} center. In this case, the hydrogen atom is able to traverse the di-iridium core without the need for swinging a terminal ligand from an equatorial site.

Hydrogen elimination from the mixed-valence cores is the microscopic reverse. In this case, reductive elimination proceeds by coupling bridging and terminal hydrides,

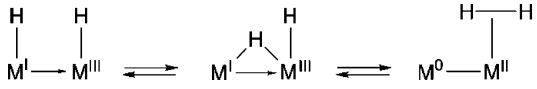

Essential for the reactivity of H_2 at M^n–M^{n+2} cores appears to be the ability of a hydrogen atom to migrate while maintaining an asymmetry of the two-electron mixed-valence core without excessive reorganization. Low-energy ligand flexing modes are important adjuncts to cooperative reactivity between metal centers because they enable the ligand to accommodate disparate coordination geometries during the course of the hydrogen atom migration. Bosnich has argued that poorly designed, inflexible ligands can forestall

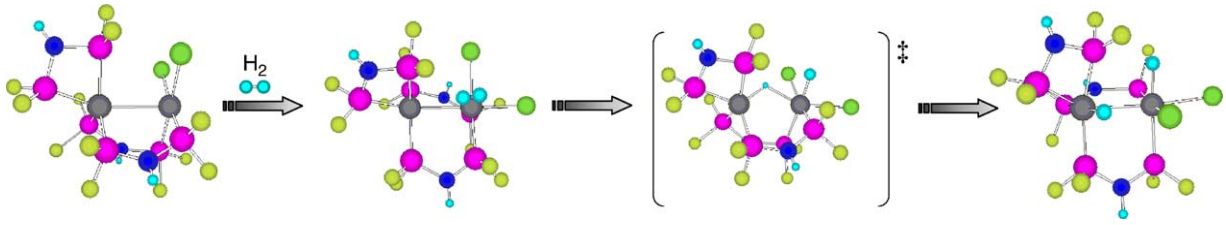

Fig. 4. Mechanistic pathway for H_2 attack and addition to an Ir^0–$Ir^{II}(X)_2$ core. The energy-minimized structures are obtained from DFT calculations. The color coding of the atoms is: Rh (gray), Cl (green), P (magenta), F (yellow), N (royal blue) and H (aquamarine).

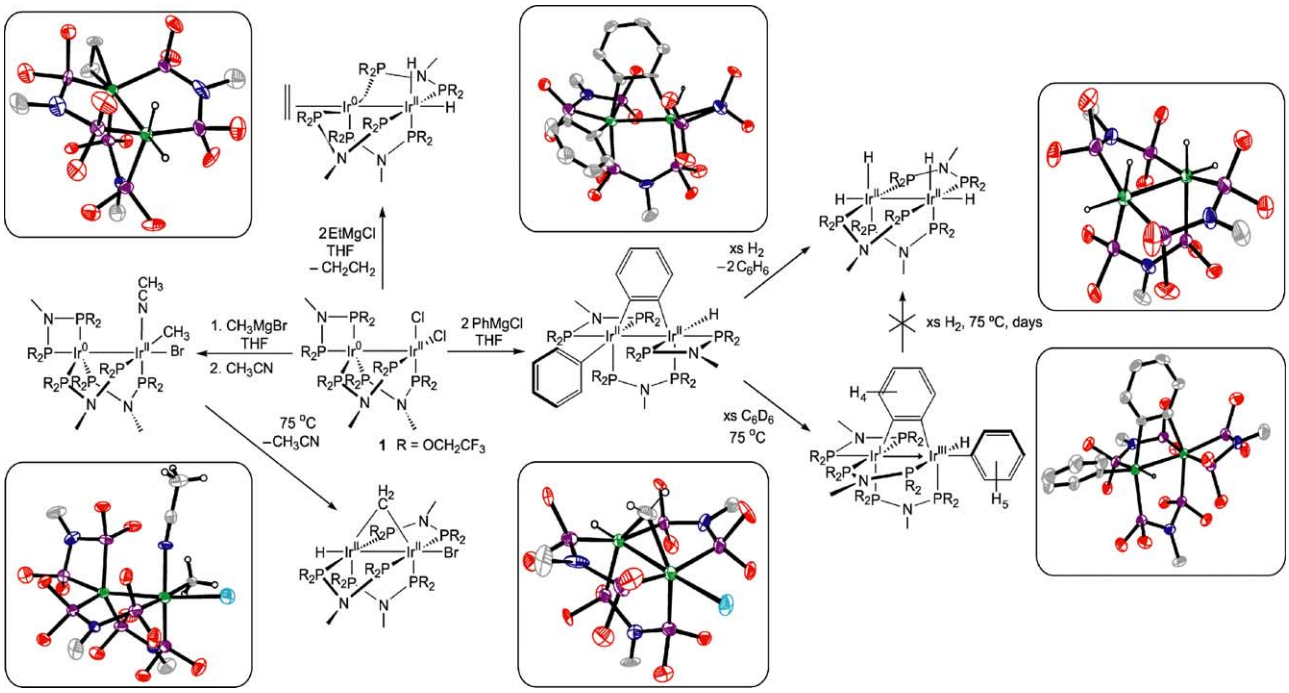

Fig. 5. Organometallic chemistry promoted by the intermetal redox cooperativity of two-electron mixed-valence complexes.

bimetallic reactivity, even without direct bonds joining the metal centers [37,38]. Our results support this contention. In addition, the diphosphazane ligand has the proper electronic properties to accommodate metals of different formal electron counts as hydrogen attacks, activates and migrates. These electronic and steric properties of the ligand appear to be advantageous, if not compulsory, to the cooperative bimetallic and reversible activation of H_2.

In the course of our investigations of H_2 and HX reactivity, we found that the intermetal two-electron redox cooperativity of M^n–M^{n+2} cores is general and applicable to the activation of other small molecules and functional groups [39]. The constellation of reactivity depicted in Fig. 5 establishes several important points: (i) two-electron mixed-valence complexes are reactive, in contrast to previous work which showed two-electron mixed valency to render complexes inert [37,38,40–44]; (ii) the M^n–M^{n+2} core is able to support hydrides of high nuclearity; and (iii) the M^n–M^{n+2} core is active towards organic substrates leading to a rich organometallic chemistry.

3. NBN coordination chemistry

The activation of the M–X bond is critical to the overall efficiency of the photocycle shown in Fig. 1. More generally, we believe that this will be the case for most HX photocatalysis schemes. We therefore sought to utilize the stronger oxidizing power of early transition metals in high oxidation states in an attempt to increase the efficiency of the kinetically and thermodynamically challenging task of photochemical halogen elimination. We were initially attracted to metalloporphyrins for H_2 photocatalysis because the *cis*-dihalide arrangement of early transition metal porphyrins is potentially conducive to X–X coupling. Additionally, metalloporphyrin systems may be expected to react rapidly with HX to produce hydrogen and the metal dihalide based on the results of early metal cyclopentadienyl complexes [45,46], which are surrogates of group IV metalloporphyrins. However, we discovered that excitation of *cis*-dihalide metalloporphyrins results in the photoreduction of the porphyrin macrocycle [47], thereby circumventing M–X photoactivation.

We have also explored whether the two-electron mixed-valence approach could be transferred to complexes of early transition metals in high oxidation states. Two-electron mixed valency in the late metal compounds described in Sections 2.1–2.3 is induced by acceptor–donor–acceptor (A–D–A) ligands in which π-accepting fluorophosphine groups are adjacent to the lone pair of an amine bridgehead. Since the phosphine groups may accept electrons from the metal or from the lone pair on the nitrogen, the ligand is able to accommodate concomitantly late metals in both low and moderate oxidation states (see Fig. 6). To stabilize early transition metals, we explored bis(alkylamido)phenylboranes, $PhB(NR)_2^{2-}$, which possess the antithetical donor–acceptor–donor (D–A–D) motif; the π-basic nature of the bisamide ligand is more suited to high valent, early transition metals. The lithiated amide derivatives of these amines were first reported in 1990 [48]; a subsequent chemistry has evolved for $PhB(NR)_2^{2-}$ complexed to main group elements [49–56]. The transition metal chemistry of these ligands, however, had been little

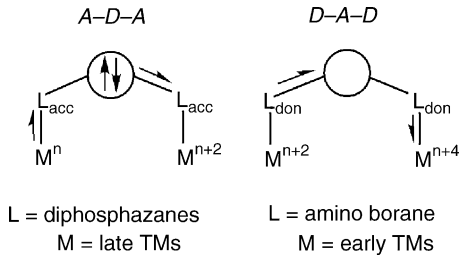

Fig. 6. Three-atom bridging ligands featuring acceptor–donor–acceptor (A–D–A) and donor–acceptor–donor (D–A–D) motifs for the electronic stabilization of two-electron mixed-valence cores.

explored, with only three such complexes reported in the literature prior to our work [48,57].

We have generalized the coordination chemistry of the $PhB(NR)_2^{2-}$ ligand by synthesizing a series of Group 4 and 5 complexes [58,59]. More importantly, we were also able to prepare the desired dimers for the Group 6 metals of molybdenum and tungsten [60]. As highlighted in Fig. 7 for the dimolybdenum complex, these metal–metal triple bond species exhibit a nearly eclipsed ligand geometry and possess the shortest metal–metal bonds of neutral M_2X_6 complexes observed to date. The strong metal-metal bond leads to a large HOMO-LUMO gap, rendering the complexes inert to oxidation. Hence a two-electron mixed-valence state may not be accessible from the metal-metal triple bond species. Even though the NBN ligand does not suit our purposes, it should find utility to other inorganic chemists as an alternative to the ever-popular amidinate ligand. The ligand demonstrates significantly shorter metal-nitrogen bonds than related amidinate ligands owing to a larger bite angle and its dianionic nature, which relaxes the need for additional ancillary anionic ligands for metal centers in high oxidation states. Additionally, the electronic and steric properties of the ligand can be tuned with substituents on both amides and by R′-substitution at the electron withdrawing B(R′) bridgehead.

4. Ligand based two-electron mixed-valence complexes

We sought to expand the design concept of two-electron mixed valency by using the ligand framework as the multi-electron/hole reservoir, instead of a bimetallic core. We turned our attention to porphyrinogens since upon oxidation of the tetrapyrrole, one or two spirocyclopropane rings (Δ) may be formed by C–C coupling between the α-carbons of neighboring pyrroles [61]. This transformation effectively stores two or four oxidizing equivalents in the macrocyclic ring. Prior to our studies, however, the generality, characterization and practical use of the ligand-based redox chemistry of porphyrinogens was hindered by the presence of redox-active axial ligands and/or polynuclear copper/iron halide counteranions [62–64]. We developed new synthetic methods that afforded the porphyrinogen with the redox inactive metal, zinc, and redox-inert and spectroscopically silent counterions. In this way we were able to unveil the redox properties

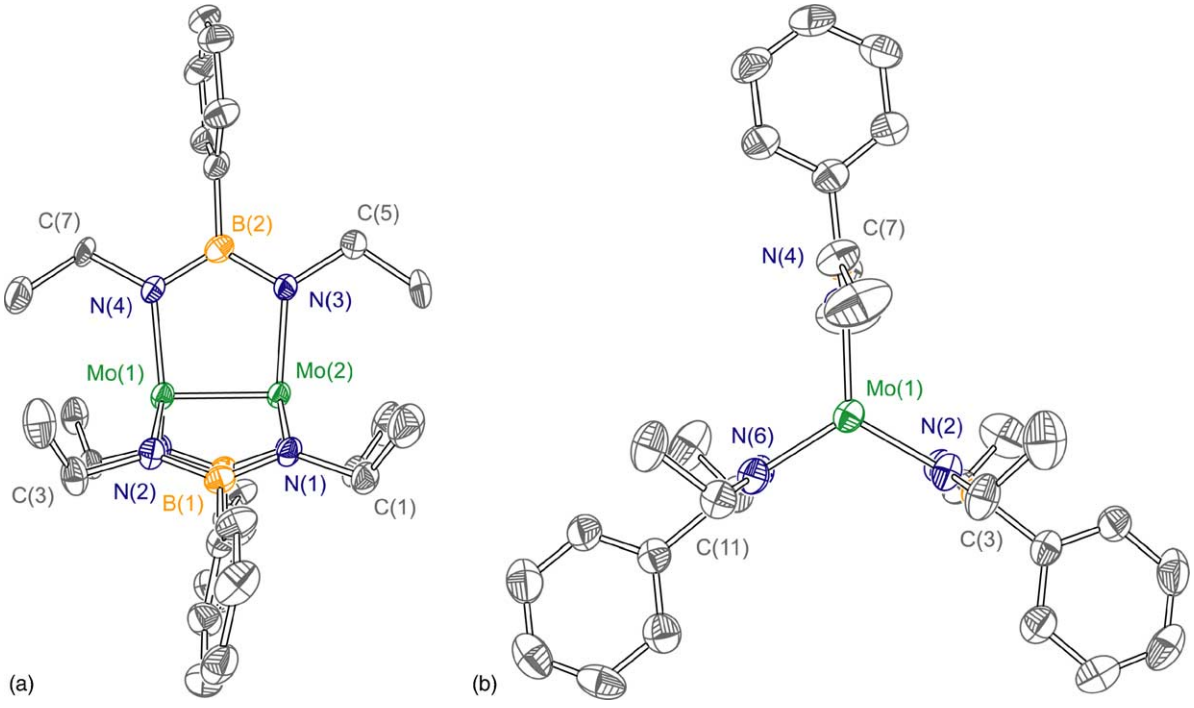

Fig. 7. Solid-state structure of $Mo_2[EtN–B^{Ph}–NEt]_3$ viewed (a) normal to and (b) along the metal–metal axis with thermal ellipsoids shown at the 30% probability level.

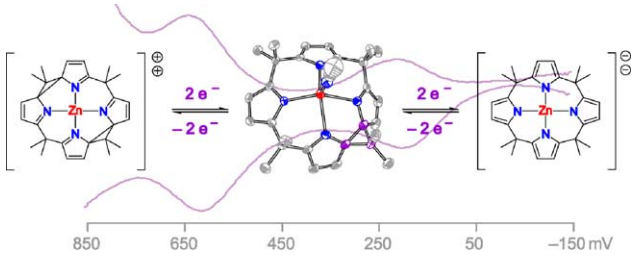

Fig. 8. Differential pulse voltammograms recorded of the porphyrinogen macrocycle coordinating the Zn(II) ion. Redox potentials are referenced vs. NHE. The solid-state structure is that of the two-electron mixed-valence intermediate (thermal ellipsoids at the 50% probability level).

of the macrocycle by electrochemistry, and isolate and characterize the three ligand oxidation states, $[LZn]^{2-}$, $[L^{\Delta}Zn]$ and $[L^{\Delta\Delta}Zn]^{2+}$ (see Fig. 8). The intermediate oxidation state, $[L^{\Delta}Zn]$, has been described theoretically and observed structurally and spectroscopically to be an ideal example of a localized two-electron mixed-valence complex [65]. DFT calculations reveal that the highest-energy occupied molecular orbitals are localized on the reduced half of the macrocycle whereas the lowest-energy unoccupied orbitals are localized on the oxidized half of the porphyrinogen. Consistent with this formulation, the intense orange color of $[L^{\Delta}Zn]$ arises from charge transfer from the reduced dipyrrole half of the macrocycle to its two-electron oxidized dipyrrole neighbor.

Scheme 4 highlights the parallel between ligand- and metal-based two-electron mixed valency. For both cases, (i) the two-electron mixed-valence intermediate is the linchpin that couples the two-electron chemistry of the individual redox centers (dipyrroles in the case of porphyrinogen, rhodium centers in the case of the bimetallic complex), (ii) the two-electron mixed-valence compound is the structural composite of the symmetric oxidized and reduced congeners and (iii) the frontier molecular orbitals and corresponding lowest energy electronic transitions are confined to the two-electron mixed-valence core. The ligand-based approach, however, differs from that of the metal-based approach in one important aspect. Since coordination geometry is inextricably linked to metal oxidation state, two-electron/hole storage in the metal-based approach must be accompanied by alterations of the primary coordination sphere. Conversely, in the approach described here, two-electron/hole storage occurs in the periphery of the macrocycle, decoupled from the acid–base chemistry of the metal. This orthogonalization between redox storage and small molecule coordination sites offers a new design element for using two-electron mixed valency to promote multielectron reactivity. Small molecule activation by this approach is contingent on relaying redox equivalents from the macrocyclic ligand to a redox-active central metal. Initial forays into this area appear promising. Using our synthetic methods, an iron porphyrinogen series has been cleanly synthesized, isolated and structurally and spectroscopically characterized. We find that the redox interplay between metal and ligand engenders an overall single step three-electron redox chemistry created between $[LFe^{III}]^{-}$ and $[L^{\Delta\Delta}Fe^{II}]^{2+}$ [66]. Studies aimed at further developing the multielectron redox chemistry of iron and other redox active metal porphyrinogens are currently in progress.

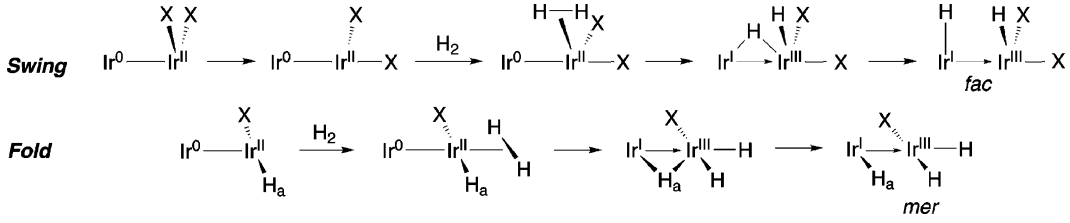

Scheme 3.

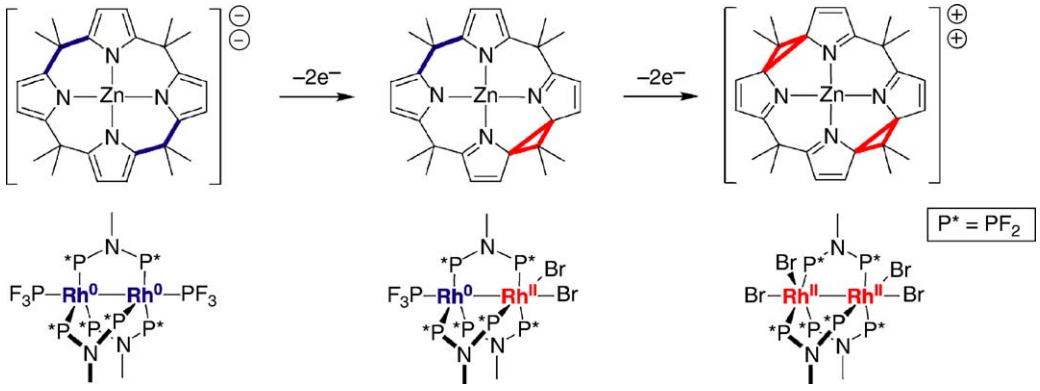

Scheme 4.

5. Di-iron(III) μ-oxo bisporphyrins for oxidative photocatalysis

5.1. Pacman porphyrins

Oxygen has been activated via a two-electron mixed-valence state by using cofacial porphyrins as photocatalysts. The synthesis of cofacial porphyrins had been previously limited to two spacers, namely, anthracene (DPA) and biphenylene (DPB) [67–72]. We have overcome the arduous synthesis of their prerequisite dialdehyde bridges by developing a novel one-pot method for obtaining xanthene and dibenzofuran bridges in high yield, allowing for the efficient gram-scale synthesis of the cofacial "Pacman" bisporphyrins bridged by xanthene (DPX) and diphenyl furan (DPD) [73–75]. By employing appropriate substituents along the periphery of the macrocyclic superstructure, it is possible to tune the pocket sizes of the Pacman motif over a series of metal-metal distances ranging from 3.5 Å to over 8.5 Å [76–79].

Our group has undertaken the first detailed studies of the electronic excited states of Pacman porphyrins [80,81]. For the case of di-iron(III) μ-oxo porphyrins, light excitation breaks the Fe^{III}–O–Fe^{III} bond to produce a (PFe^{II})(PFe^{IV}=O) cofacial intermediate, which oxidizes simple electron-rich substrates [79,82], such as phosphines and sulfides [83,84]. Reaction of two ferrous porphyrin subunits with O_2 reforms the di-iron(III) μ-oxo complex, presumably by a modified Balch mechanism [85,86] for reentry into the catalytic cycle. A general depiction of this cycle appears in Fig. 9. This oxidative photocatalysis builds on the chemistry of unbridged $Fe_2^{III,III}$ μ-oxo porphyrins [87–92] with the twist that the DPD framework is structurally "spring-loaded" [93], resulting from the unprecedented ability of the cofacial porphyrin to open and close its binding pocket by a vertical distance of over 4 Å (Fig. 9, top). The vertical flexibility of the DPD cleft gives rise to an efficient oxygen atom transfer (OAT) photochemistry. Comparative photochemical studies of spring-loaded (DPD)Fe_2O and non spring-loaded (DPX)Fe_2O (DPX = xanthene spacer, relaxed pocket ~3.7 Å) Pacman architectures have revealed a superior photoreactivity (ca. 10,000-fold) of the former. Additionally, the DPX Pacman congener is far more sensitive to the size (cone angle) of the attacking substrate [79]. The mechanistic details of the OAT photocycle were investigated by transient absorption spectroscopy [93]. Rates of net OAT for spring-loaded DPD Pacman platforms are four orders of magnitude greater than those of relaxed platforms. Transient spectroscopy measurements show that the spring action of the bisporphyrin cleft does little to impede re-clamping to form the μ-oxo species but rather is manifest to opening the cofacial cleft to allow substrate access to the photogenerated ferryl oxidant (Fig. 10). These studies have shown that Pacman porphyrins afford a unique combination of synthetic availability and vertical flexibility. These attributes are important because (i) two-electron mixed valency is used to drive two-electron oxi-

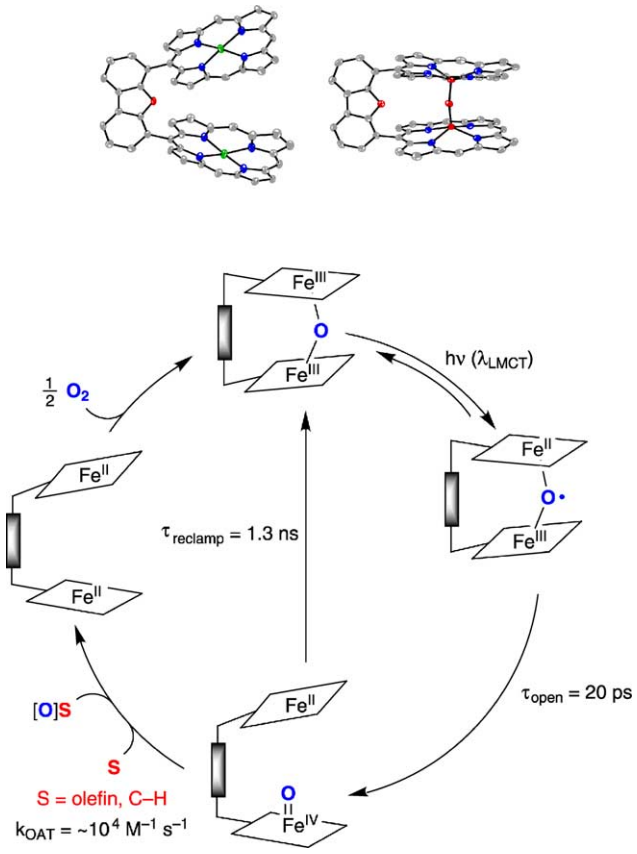

Fig. 9. Structural illustration of the Pacman effect for DPD cofacial porphyrins (top) and its spring-action for use in the construction of a photocatalytic oxidation cycle (bottom).

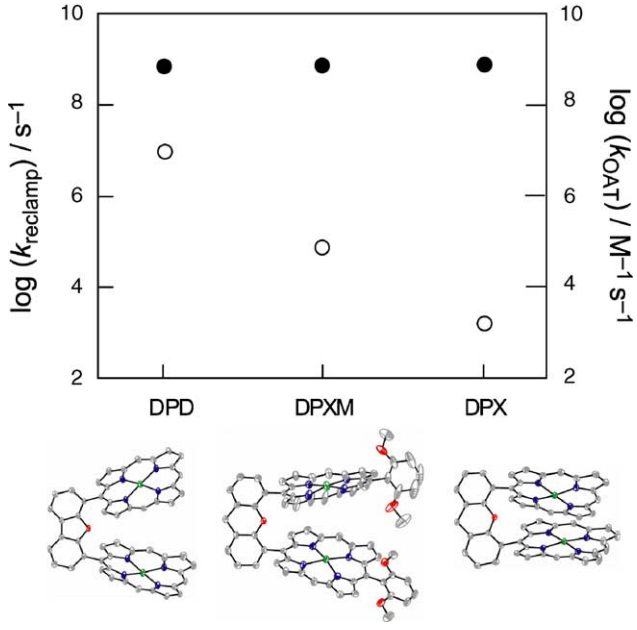

Fig. 10. The rates for $k_{reclamp}$ (●) and k_{OAT} (○) for the photocycle shown in Fig. 9 for oxidation of $P(OMe)_3$ by cofacial bisporphyrins of varying cleft dimensions: d_{M-M}(relaxed) = 7.775 Å (DPD), 5.913 Å (DPXM), and 3.708 Å (DPX).

dations, (ii) the multielectron process is photocatalytic under mild conditions and (iii) the photo-oxidation proceeds without the need for an external co-reductant and uses dioxygen as the terminal oxidant and oxygen atom source.

5.2. Fluorinated Pacman porphyrins

Whereas Pacman etioporphyrin architectures oxidize electron-rich organic substrates (i.e., phosphines and sulfides) [82], photo-oxidation of more thermodynamically challenging substrates (i.e., olefins, alkanes, amines, etc.) is not facile owing to the modest redox potential of the etioporphyrin ferryl subunit [79,94]. It is well established that the oxidizing power of metalloporphyrins is enhanced by introducing electron-withdrawing groups onto the porphyrin periphery [95,96]. In accordance with this property of porphyrins, the spring-loaded DPD platform appended with *meso*-pentafluorophenyl porphyrins (DPDF) is an active catalyst for the photoinduced aerobic oxygenation of sulfides and olefins under mild conditions and with the highest turnover numbers (TONs) yet achieved for a cofacial bisporphyrin photocatalyst [97]. The electron deficiency of the fluorinated porphyrin results in a red-shift of the absorption spectrum, allowing us to use relatively long-wavelength light for photolysis (λ_{exc} = 425–460 nm). This is in contrast with the far less oxidizing *etio*porphyrin DPD Pacman architecture discussed above, which requires light in the near UV region (λ_{exc} = 360–380 nm). The photoreaction is exceptionally clean and we have succeeded in executing the photocatalysis with turnover numbers exceeding 1000. We have also observed that (DPDF)Fe_2O can convert easily oxidized alkanes to alcohols or ketones, as the Pacman porphyrin photocatalyzes the oxygenation of dihydroanthracene and diphenylmethane with TONs of 200–300. The oxidation of hydrocarbons by O_2 without the need for an external co-reductant is noteworthy and thus is a photochemistry of fundamental interest. Two immediate goals are to broaden the substrate scope and increase the overall efficiency of the process.

6. Conclusions

A rational framework for advancing the multielectron photochemistry of new metal complexes has been developed using two-electron mixed-valence complexes as the redox platform. The excited-state chemistry of these compounds offers an interesting alternative to the conventional one-electron photochemistry that has been studied in detail for several decades. Initial forays into the study of two-electron mixed valency in transition metal complexes have opened new avenues for effecting multielectron photocatalysis. To date, we have successfully activated hydrogen and oxygen and have shown that it is possible to construct photocycles for H_2 production from protic media, as well as OAT using O_2 as the terminal oxidant and oxygen atom source. The different classes of complexes (Scheme 1) that perform these tasks share basic commonalities that are intrinsic to the two-electron mixed-valence design: (i) the two-electron mixed-valence intermediate is the linchpin that couples the two-electron chemistry of the individual redox centers; (ii) inter-site redox cooperativity is essential to managing the observed multielectron chemistry; (iii) ligand frameworks must exhibit an electronic and vibrational plasticity [98] so as to accommodate the disparate coordination geometries that are attendant to multielectron changes in formal oxidation states of the redox centers; and (iv) M–X (X = halogen, oxygen) bonds must be activated by photoexcitation to enable photocycles to be closed. Indeed, additional systems that take advantage of these foregoing principles should be of continued interest to the inorganic chemist, particularly with respect to the development of photochemical cycles concerned with the activation of small molecules of energy consequence.

Acknowledgment

J.R. thanks the Fannie and John May Hertz Foundation for a pre-doctoral fellowship. J.B. gratefully acknowledges MIT for a pre-doctoral Presidential Fellowship, and Shell Oil Company for fellowship funding. J.L.D. thanks the MIT Undergraduate Research Opportunities Program (UROP) for support. T.G.G. acknowledges a postdoctoral fellowship from the National Institutes of Health. This work was supported by the National Science Foundation (CHE-0132680).

References

[1] Basic Research Needs for the Hydrogen Economy, in: M. Dresselhaus (Ed.), Report of the Basic Energy Sciences Workshop on Hydrogen Production, Storage, and Use, Argonne National Laboratory, U.S. Department of Energy, Washington, DC, 13–15 May 2003.
[2] D.G. Nocera, Chem. Eng. News 79 (2001) 250.
[3] D.G. Nocera, Acc. Chem. Res. 28 (1995) 209.
[4] D.G. Nocera, J. Clus. Sci. 5 (1994) 185.
[5] R.I. Cukier, D.G. Nocera, Annu. Rev. Phys. Chem. 49 (1998) 337.
[6] J. Stubbe, D.G. Nocera, C.S. Yee, M.C.Y. Chang, Chem. Rev. 103 (2003) 2167.
[7] C. Turró, C.K. Chang, G.E. Leroi, R.I. Cukier, D.G. Nocera, J. Am. Chem. Soc. 114 (1992) 4013.
[8] J.A. Roberts, J.P. Kirby, D.G. Nocera, J. Am. Chem. Soc. 117 (1995) 8051.
[9] J.P. Kirby, N.A. van Dantzig, C.K. Chang, D.G. Nocera, Tetrahedron Lett. 36 (1995) 3477.
[10] Y. Deng, J.A. Roberts, S.M. Peng, C.K. Chang, D.G. Nocera, Angew. Chem. Int. Ed. Engl. 36 (1997) 2124.
[11] J.P. Kirby, J.A. Roberts, D.G. Nocera, J. Am. Chem. Soc. 119 (1997) 9230.
[12] J.A. Roberts, J.P. Kirby, S.T. Wall, D.G. Nocera, Inorg. Chim. Acta 263 (1997) 395.
[13] C.Y. Yeh, S.E. Miller, S.D. Carpenter, D.G. Nocera, Inorg. Chem. 40 (2001) 3643.
[14] N.H. Damrauer, J.M. Hodgkiss, J. Rosenthal, D.G. Nocera, J. Phys. Chem. B 108 (2004) 6315.
[15] C.J. Chang, M.C.Y. Chang, N.H. Damrauer, D.G. Nocera, Biophys. Biochim. Acta 1655 (2004) 13.

[16] C.J. Chang, Z.-H. Loh, C. Shi, F.C. Anson, D.G. Nocera, J. Am. Chem. Soc. 126 (2004) 10013.
[17] C.J. Chang, L.L. Chng, D.G. Nocera, J. Am. Chem. Soc. 125 (2003) 1866.
[18] L.L. Chng, C.J. Chang, D.G. Nocera, Org. Lett. 5 (2003) 2421.
[19] C.Y. Yeh, C.J. Chang, D.G. Nocera, J. Am. Chem. Soc. 123 (2001) 1513.
[20] A. Vogler, A.H. Osman, H. Kunkely, Coord. Chem. Rev. 64 (1985) 159.
[21] T.J. Meyer, Prog. Inorg. Chem. 30 (1983) 389.
[22] R.J. Haines, E. Meintjies, M. Laing, Inorg. Chim. Acta 36 (1979) L403.
[23] T.G. Gray, D.G. Nocera, Chem. Commun. (2005) 1540.
[24] A.F. Heyduk, A.M. Macintosh, D.G. Nocera, J. Am. Chem. Soc. 121 (1999) 5023.
[25] A.L. Odom, A.F. Heyduk, D.G. Nocera, Inorg. Chim. Acta 297 (2000) 330.
[26] A.F. Heyduk, D.G. Nocera, J. Am. Chem. Soc. 122 (2000) 9415.
[27] A.F. Heyduk, D.G. Nocera, Chem. Commun. (1999) 1519.
[28] A.S. Veige, D.G. Nocera, Chem. Commun. (2004) 1958.
[29] J. Kadis, Y.-g.K. Shin, J.I. Dulebohn, D.L. Ward, D.G. Nocera, Inorg. Chem. 35 (1996) 811.
[30] A.F. Heyduk, D.J. Krodel, E.E. Meyer, D.G. Nocera, Inorg. Chem. 41 (2002) 634.
[31] J.I. Dulebohn, D.L. Ward, D.G. Nocera, J. Am. Chem. Soc. 112 (1990) 2969.
[32] J.I. Dulebohn, D.G. Nocera, J. Am. Chem. Soc. 110 (1988) 4054.
[33] A.F. Heyduk, D.G. Nocera, Science 293 (2001) 1639.
[34] A.J. Esswein, A.S. Veige, D.G. Nocera, J. Am. Chem. Soc., submitted for publication.
[35] T.G. Gray, A.S. Veige, D.G. Nocera, J. Am. Chem. Soc. 126 (2004) 9760.
[36] A.S. Veige, T.G. Gray, D.G. Nocera, Inorg. Chem. 44 (2005) 17.
[37] B. Bosnich, Inorg. Chem. 38 (1999) 2554.
[38] D.G. McCollum, B. Bosnich, Inorg. Chim. Acta 270 (1998) 13.
[39] A.S. Veige, A.J. Esswein, D.G. Nocera, Organometallics, submitted for publication.
[40] A.L. Gavrilova, B. Bosnich, Chem. Rev. 104 (2004) 349.
[41] T.G. Schenck, J.M. Downes, C.R.C. Milne, P.B. Mackenzie, H. Boucher, J. Whelan, B. Bosnich, Inorg. Chem. 24 (1985) 2334.
[42] T.G. Schenck, C.R.C. Milne, J.F. Sawyer, B. Bosnich, Inorg. Chem. 24 (1985) 2338.
[43] J. Halpern, Inorg. Chim. Acta 62 (1982) 31.
[44] J. Halpern, B.L. Goodall, G.P. Khare, H.S. Lim, J.J. Pluth, J. Am. Chem. Soc. 97 (1975) 2301.
[45] K. Shibata, T. Aida, S. Inoue, Chem. Lett. (1992) 1171.
[46] P.C. Wailes, H. Weigold, J. Organomet. Chem. 2 (1970) 405.
[47] B.J. Pistorio, D.G. Nocera, J. Photochem. Photobiol. A 162 (2004) 563.
[48] D. Fest, C.D. Habben, A. Meller, G.M. Sheldrick, D. Stalke, F. Pauer, Chem. Ber. 123 (1990) 703.
[49] T. Albrecht, G. Elter, M. Noltemeyer, A. Meller, Z. Anorg. Allg. Chem. 624 (1998) 1514.
[50] M. Geschwentner, M. Noltemeyer, G. Elter, A. Meller, Z. Anorg. Allg. Chem. 620 (1994) 1403.
[51] T. Chivers, X. Gao, M. Parvez, Angew. Chem. Int. Ed. Engl. 34 (1995) 2549.
[52] C.D. Habben, A. Heine, G.M. Sheldrick, D. Stalke, Z. Naturforsch. 47b (1992) 1367.
[53] C.D. Habben, A. Heine, G.M. Sheldrick, D. Stalke, M. Bühl, P.v.R. Schleyer, Chem. Ber. 124 (1991) 47.
[54] C.D. Habben, R. Herbst-Irmer, M. Noltemeyer, Z. Naturforsch. 46b (1991) 625.
[55] A. Heine, D. Fest, D. Stalke, C.D. Habben, A. Meller, G.M. Sheldrick, J. Chem. Soc., Chem. Commun. (1990) 742.
[56] H.-J. Koch, H.W. Roesky, S. Besser, R. Herbst-Irmer, Chem. Ber. 126 (1993) 571.
[57] H.-J. Koch, H.W. Roesky, R. Bohra, M. Noltemeyer, H.-G. Schmidkt, Angew. Chem. Int. Ed. Engl. 31 (1992) 598.
[58] D.R. Manke, O.T.P. Bush, D.G. Nocera, Inorg. Chim. Acta 345 (2003) 235.
[59] D.R. Manke, D.G. Nocera, Inorg. Chem. 42 (2003) 4431.
[60] D.R. Manke, Z.-H. Loh, D.G. Nocera, Inorg. Chem. 43 (2004) 3618.
[61] C. Floriani, R. Floriani-Moro, in: K. Kadish, K.M. Smith, R. Guilard (Eds.), The Porphyrin Handbook, vol. 3, Academic Press, San Diego CA, 2000, p. 405, Chapter 25.
[62] R. Crescenzi, E. Solari, C. Floriani, A. Chiesi-Villa, C. Rizzoli, J. Am. Chem. Soc. 116 (1994) 5691.
[63] S. De Angelis, E. Solari, C. Floriani, A. Chies-Villa, C. Rizzoli, J. Am. Chem. Soc. 116 (1994) 5702.
[64] R. Crescenzi, E. Solari, C. Floriani, A. Chiesi-Villa, C. Rizzoli, J. Am. Chem. Soc. 121 (1999) 1695.
[65] J. Bachmann, D.G. Nocera, J. Am. Chem. Soc. 126 (2004) 2829.
[66] J. Bachmann, D.G. Nocera, J. Am. Chem. Soc. 127 (2005) 4730.
[67] J.P. Collman, J.E. Hutchinson, M.A. Lopez, A. Tabard, R. Guilard, W.K. Seok, J.A. Ibers, M. L'Her, J. Am. Chem. Soc. 114 (1992) 9869.
[68] R. Guilard, M.A. Lopez, A. Tabard, P. Richard, C. Lecomte, S. Brandes, J.E. Hutchinson, J.P. Collman, J. Am. Chem. Soc. 114 (1992) 9877.
[69] J.P. Collman, P.S. Wagenknecht, J.E. Hutchison, Angew. Chem. Int. Ed. Engl. 33 (1994) 1537.
[70] C.K. Chang, I. Abdalalmuhdi, J. Org. Chem. 48 (1983) 5388.
[71] C.K. Chang, I. Abdalmuhdi, Angew. Chem. Int. Ed. Engl. 23 (1984) 164.
[72] C.K. Chang, H.Y. Liu, I. Abdalmuhdi, J. Am. Chem. Soc. 106 (1984) 2725.
[73] Y. Deng, C.J. Chang, D.G. Nocera, J. Am. Chem. Soc. 122 (2000) 410.
[74] C.J. Chang, Y. Deng, A.F. Heyduk, C.K. Chang, D.G. Nocera, Inorg. Chem. 39 (2000) 959.
[75] C.J. Chang, Y. Deng, C. Shi, C.-K. Chang, F.C. Anson, D.G. Nocera, Chem. Commun. (2000) 1355.
[76] L.L. Chng, C.J. Chang, D.G. Nocera, J. Org. Chem. 68 (2003) 4075.
[77] C.J. Chang, Y. Deng, S.M. Peng, G.H. Lee, C.Y. Yeh, D.G. Nocera, Inorg. Chem. 41 (2002) 3008.
[78] C.J. Chang, C.-Y. Yeh, D.G. Nocera, J. Org. Chem. 67 (2002) 1403.
[79] C.J. Chang, E.A. Baker, B.J. Pistorio, Y. Deng, Z.-H. Loh, S.E. Miller, S.D. Carpenter, D.G. Nocera, Inorg. Chem. 41 (2002) 3102.
[80] Z-H. Loh, S.E. Miller, C.J. Chang, S.D. Carpenter, D.G. Nocera, J. Phys. Chem. A 106 (2002) 11700.
[81] C.J. Chang, Z-H. Loh, Y. Deng, D.G. Nocera, Inorg. Chem. 42 (2003) 8262.
[82] B.J. Pistorio, C.J. Chang, D.G. Nocera, J. Am. Chem. Soc. 124 (2002) 7884.
[83] R.H. Holm, Chem. Rev. 87 (1987) 1401.
[84] R.H. Holm, J.P. Donahue, Polyhedron 12 (1993) 571.
[85] D-H. Chin, J. Del Gaudio, G.N. La Mar, A.L. Balch, J. Am. Chem. Soc. 99 (1977) 5486.
[86] D-H. Chin, G.N. La Mar, A.L. Balch, J. Am. Chem. Soc. 102 (1980) 4344.
[87] M.W. Peterson, D.S. Rivers, R.M. Richman, J. Am. Chem. Soc. 107 (1985) 2907.
[88] M.W. Peterson, R.M. Richman, Inorg. Chem. 24 (1985) 722.
[89] L. Weber, R. Hommel, J. Behling, G. Haufe, H. Hennig, J. Am. Chem. Soc. 116 (1994) 2400.
[90] L. Weber, G. Haufe, D. Rehorek, H. Hennig, Chem. Commun. (1991) 502.
[91] D.N. Hendrickson, M.G. Kinnaird, K.S. Suslick, J. Am. Chem. Soc. 109 (1987) 1243;
G. Ferraudi, K.S. Suslick, J. Am. Chem. Soc. 109 (1987) 1243.

[92] C.R. Guest, K.D. Straub, J.A. Hutchinson, P.M. Rentzepis, J. Am. Chem. Soc. 110 (1988) 5276.
[93] J.M. Hodgkiss, C.J. Chang, B.J. Pistorio, D.G. Nocera, Inorg. Chem. 42 (2003) 8270.
[94] B.J. Pistorio, C.J. Chang, D.G. Nocera, J. Am. Chem. Soc. 124 (2002) 7884.
[95] S. Neya, N. Funasaki, J. Heterocyclic Chem. 34 (1997) 689.
[96] E.K. Woller, S.G. DiMagno, J. Org. Chem. 62 (1997) 1588.
[97] J. Rosenthal, B.J. Pistorio, L.L. Chng, D.G. Nocera, J. Org. Chem. 70 (2004) 1885.
[98] For further insights into chemical plasticity see: http://chem.berkeley.edu/people/faculty/chang/chang.html.